EUROFUSION WPDTT2-PR(16) 16242

A. Lampasi et al.

The DTT device: power supplies and electrical distribution system

Preprint of Paper to be submitted for publication in
Fusion Engineering and Design

This work has been carried out within the framework of the EUROfusion Consortium and has received funding from the Euratom research and training programme 2014-2018 under grant agreement No 633053. The views and opinions expressed herein do not necessarily reflect those of the European Commission.

Available online at www.sciencedirect.com

ScienceDirect

ELSEVIER

The DTT device: power supplies and electrical distribution system

Alessandro Lampasi [a*], Pietro Zito [a], F. Starace [a], P. Costa [a], G. Maffia [a], S. Minucci [b], E. Gaio [c], V. Toigo [c], L. Zanotto [c], S. Ciattaglia [d]

[a] *National Agency for New Technologies, Energy and Sustainable Economic Development (ENEA), Frascati, Italy*
[b] *University of Naples Federico II, Naples, Italy*
[c] *Consorzio RFX, Padova, Italy*
[d] *EUROfusion Consortium, Garching, Germany*

Abstract

This paper presents the design criteria and the preliminary characteristics of the power supply and electrical systems of the Divertor Tokamak Test (DTT) facility. The power supply system has to feed: 6 superconducting modules of the central solenoid, 6 poloidal field superconducting coils, 18 toroidal field superconducting coils designed for a current up to 50 kA, some coils for plasma fast control and vertical stabilization, the electron (ECRH) and ion (ICRH) cyclotron additional heating systems for about 25 MW delivered to the plasma, further 20 MW to the plasma by a neutral beam injector (NBI) and all the auxiliary systems and services.
The analysis was carried out on a reference scenario with a plasma current of 6 MA, mainly to estimate the electrical power needed to operate the facility, but also to identify some design choices and component ratings.

Keywords: Divertor Tokamak Test (DTT), power supply, AC/DC converter, inverter, Switching Network Unit (SNU), Fast Discharge Unit (FDU), quench protection, high power delivery.

1. Introduction

The management of the heat exhaust is one of the most challenging problems for the realization of fusion energy. The European roadmap proposes a Divertor Tokamak Test (DTT) facility to address such a problem [1]. This facility is conceived as a test bed for the conventional and alternative solutions for the divertor systems that could be introduced in ITER and extrapolated to DEMO. However, in the present proposal, DTT will be a complete tokamak that requires comprehensive power supply (PS) and electrical systems to feed the magnetic field coils, the additional heating systems and the auxiliary services [2-7].

Fig. 1 shows an overview of the DTT plasma configuration and main coils. The coil positions and cross-sections were designed with an iterative procedure taking into account the plasma specifications as well as the geometrical and financial constraints [8, 9].

The DTT PS system has to feed (see also Fig. 1):

- The central solenoid (CS) divided in 6 superconducting modules (CS3U, CS2U, CS1U, CS1L, CS2L, CS3L), each with an independent PS circuit;
- 6 poloidal field superconducting coils (PFCs), classified as PF1, PF2, PF3, PF4, PF5, PF6.
- 18 toroidal field superconducting coils (TFCs), designed to operate with a current up to 50 kA.
- Some fast plasma control coils, including at least two non-superconducting internal coils (IC5 and IC6) for plasma vertical stabilization.
- The electron (ECRH) and ion (ICRH) cyclotron additional heating (and current drive) systems, for about 25 MW delivered to the plasma [10, 11].
- All the auxiliary systems and services.
- An upgrade of the heating system, able to deliver further 20 MW to the plasma, especially by a neutral beam injector (NBI) [10, 12].

This paper presents the conceptual design and the preliminary characteristics of the DTT PSs and electrical systems. The analysis was carried out mainly to estimate the electrical power needed to operate the facility, but also to identify some design choices and component ratings.

The calculations were performed on a reference single null scenario (plasma current I_p=6 MA), that is expected to be the most demanding one in terms of electrical power and stress on the components. The experiment duty cycle for this scenario is expected to be 100s/3600s.

Due to the importance of realizing the DTT scopes respecting the time schedule and budget constraints [9], the general principle for the preliminary design was to identify and select solutions ensuring a good technological feasibility confidence. Some promising alternative solutions or improvements have already been identified and will be investigated in parallel with the main project.

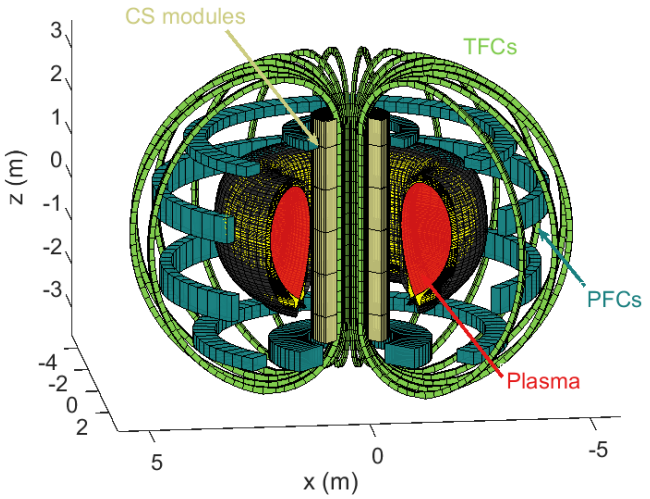

Fig. 1. 3-D view of the DTT coil and plasma shape during a typical single null configuration.

The voltages and currents to be provided by the coil PSs were estimated by applying the reference scenario in terms of current evolution in each coil to the magnetically coupled circuits model, taking into account the switching network unit (SNU) contributions [13]. While the CS, PFC and IC powers must be estimated together because of their mutual interactions, the other contributions can be considered as rather independent.

Even if the heating systems will be upgraded in successive phases [10], the power contribution related to the additional heating systems was estimated for the maximum expected peak value.

At the present stage of the project, there are not good enough details to model some contributions, such as power supply system for controlling error field or magnetohydrodynamic (MHD) instabilities. Moreover, the control of the local magnetic configuration close to the divertor target will be obtained by a special set of internal coils [8]. However, the experience gained on other tokamaks teaches that the involved power levels have a limited impact on the overall ratings [14].

For this reason and for other model approximations, but also in order to allow modifications and future upgrades, a reasonable increment is applied to the results of the power estimation.

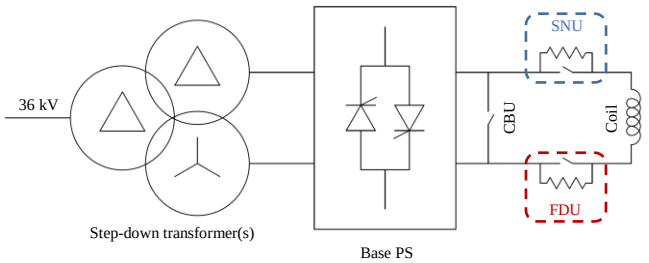

Fig. 2. General scheme of a CS or PFC PS circuit.

2. Poloidal power supply systems

2.1. Circuital configurations

The PS system of each CS and PF circuit consists of:

1. A step-down transformer (from medium voltage at 36 kV to low voltage below 1 kV) optimized to supply the downstream converters. Due to the need to obtain 12-pulse operations, the transformer could be implemented either by two secondary windings or by splitting it in two separated transformers.
2. A Base PS containing at least two AC/DC converters based on thyristor bridges. The two converters operate with a 30° phase displacement to obtain a 12-pulse waveform. As shown in Fig. 2, each switch is composed of two back-to-back thyristors to implement 4-quadrant operations.
3. A crowbar unit (CBU) to by-pass the Base PS and the load in case of fault [15].
4. A commutation system, that is a SNU in most of the cases or a simple by-pass switch (BPS) for the PF3 and PF4 coils.
5. A fast discharge unit (FDU) able to insert a resistor in the circuit when it is necessary to discharge the magnetic energy stored in the load coil (especially for superconducting quench protection) [16].

2.2. SNUs, FDUs and BPSs

Since the Base PSs are not able to produce the abrupt current derivative required to initiate and sustain the plasma breakdown, a SNU is inserted in each CS and PFC circuit. This general scheme is valid for every CS and PF coil, with the exception of the two coils PF3 and PF4, as they have a BPS instead of the SNU that is closed after the plasma breakdown.

Both the SNUs and the FDUs are based on fast switching of high DC currents. Good performances and repeatability are expected thanks to the idea of using a hybrid switch already explored for JT-60SA [13, 16]. The inadequate velocity and repeatability of the main electromechanical BPS is virtually hidden by some parallel electronic static devices. The same devices improve the expected BPS lifecycle and reliability by limiting the arc phenomena [10]. However, the SNUs and the FDUs have different functions and required performances. For instance, a SNU needs to perform two successive operations (opening and closing sequences) in every plasma experiment.

The values of the SNU resistances and of the consequent breakdown voltages are identified with the procedure presented in next section. The obtained values are feasible and quite homogenous.

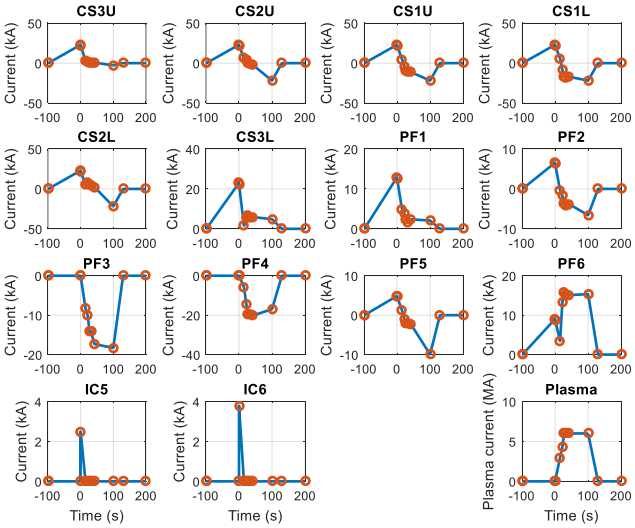

Fig. 3. Reference current scenario for the poloidal field coils and for the plasma. The red circles represent the 12 defined time instants.

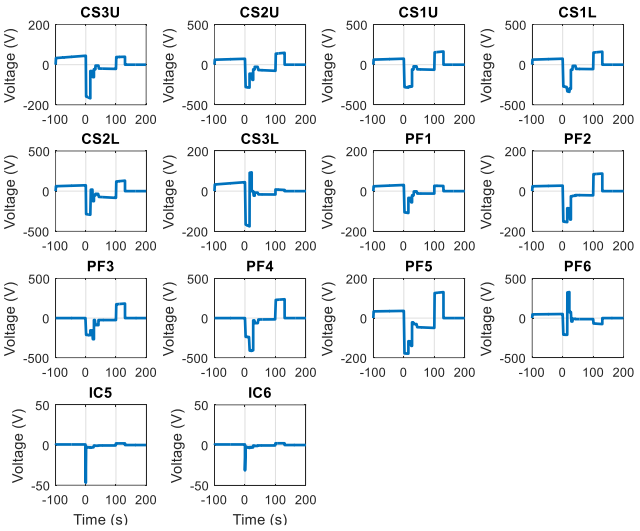

Fig. 6. Voltage to be produced by each Base PS to achieve the current scenario in Fig. 3.

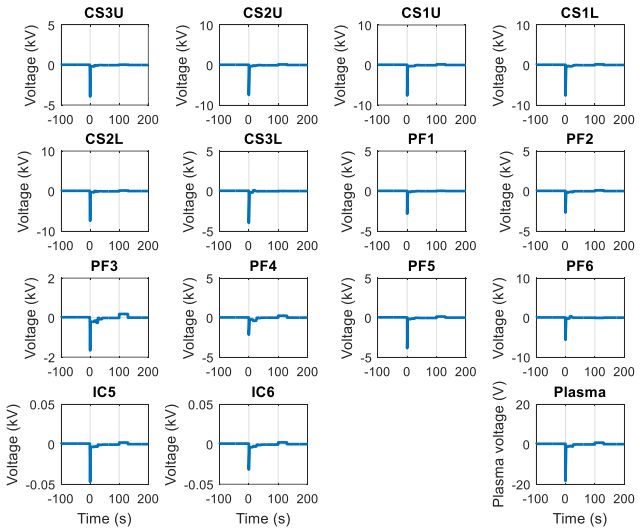

Fig. 4. Coil and plasma voltages for the current reference scenario in Fig. 3.

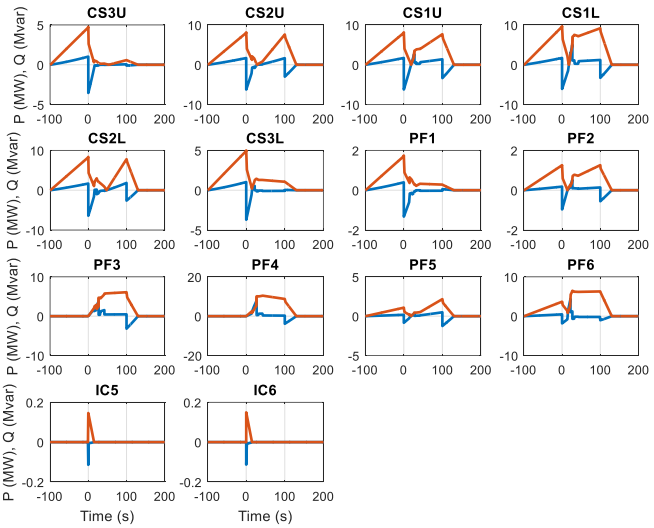

Fig. 7. Active (blue curves) and reactive (red curves) powers for each coil PS producing the reference scenario.

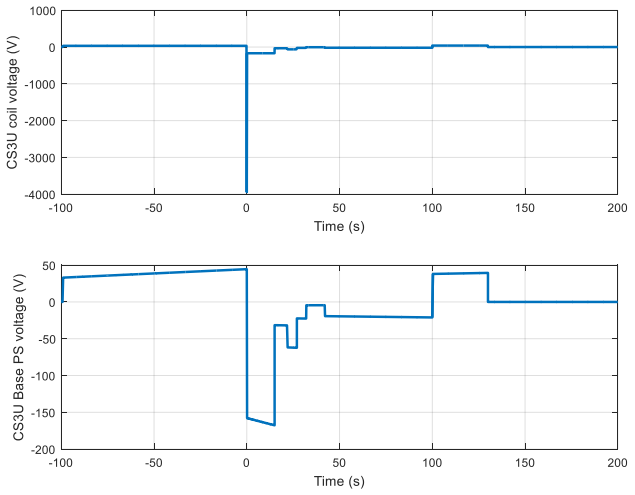

Fig. 5. Comparison between the voltage across the coil terminals and the voltage to be produced by the Base PS for the CS3U module.

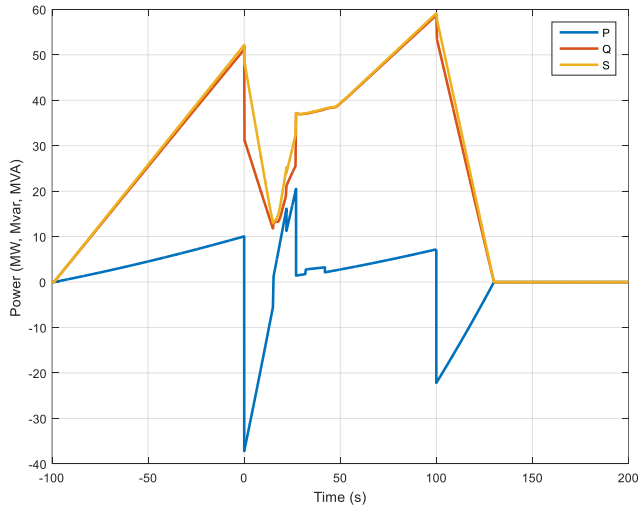

Fig. 8. Total active, reactive and apparent power for the CS, PF and IC PS systems.

2.3. Coil functional models and numerical results

The design moved from a reference scenario defined in terms of time evolution of the coil currents to estimate successively the coil voltages, the Base PS voltages and the active and reactive powers. The numerical data are based on the 6 MA reference scenario that is the most demanding one in terms of electrical power. The currents in this scenario are shown in Fig. 3.

The profiles reported in Fig. 3 for the IC5 and IC6 currents are only examples, as the actual ones depend on the plasma evolution. More pulses with the same shapes are expected in the practical cases. While this have a limited impact in terms of power, the presented curves are useful to assess the PS current and voltage ratings.

The DTT experiments are described by the current scenarios, consisting in the profiles of the coil currents versus time for each supplied poloidal coil (6 CS modules, 6 EF coils, 2 ICs). The solution of the MHD problem provides also the behavior of plasma current for the given scenarios.

Therefore, a current scenario is fully characterized by a time-dependent vector $\underline{I}(t)$ with order 15×1 (14 coils and the plasma) including at least the current samples for the N time instants $t_1, t_2, \ldots, t_n, \ldots, t_N$ when the currents are defined. The values of $\underline{I}(t)$ are emphasized as red circles in Fig. 3 for the reference scenario with N=12. Even though the scenario is defined by few samples, the waveforms are oversampled for a better numerical approximation. The first 14 rows of $\underline{I}(t)$ gives the vector $\underline{I}_{\text{coil}}(t)$ of the currents flowing in the 14 coils, the last row contains the plasma current $I_p(t)$.

The magnetic interactions among the elements of the tokamak cross-section are characterized by a square and symmetric 15×15 inductance matrix $\underline{\underline{M}}$. This matrix contains at least the mutual inductances among the supplied (active) coils and between these coils and the plasma current. A more refined model should include the parameters of the "passive" elements of the tokamak in the matrix $\underline{\underline{M}}$. The lack of these parameters at this stage is expected to be compensated by the safety margins introduced in the final results.

The entries in the main diagonal of $\underline{\underline{M}}$ correspond to the self-inductance of each coil and are about 78 mH or 154 mH for the CS modules, with a maximum of about 340 mH for PF4.

Analogously to $\underline{I}_{\text{coil}}(t)$, it is possible to define a voltage vector $\underline{V}_{\text{coil}}(t)$ having order 14×1 containing the time evolution of the voltage across the two terminals of each of the 14 coils when the scenario currents flow through them. A further vector $\underline{V}(t)$ with order 15×1 can be obtained by reporting the plasma loop voltage in the last row. The $\underline{V}(t)$ corresponding to a current scenario $\underline{I}(t)$ can be calculated by applying the formula:

$$\underline{V}(t) = \underline{\underline{M}} \frac{d\underline{I}(t)}{dt}. \quad (1)$$

Fig. 4 shows the voltages across the two terminals of the coils and for the plasma loop for the current scenario shown in Fig. 3.

2.4. Average models and results for the PS systems

The voltage across the coil terminals $\underline{V}_{\text{coil}}(t)$ is simply given by the first 14 rows of $\underline{V}(t)$. The actual average voltage $\underline{V}_{\text{PS}}(t)$ to be produced by the PS systems should account also for the voltage drops in the circuit (DC bus bars, cryogenic transitions, connections, joints, parasitic effects, SNUs and so on):

$$\underline{V}_{\text{PS}}(t) = \underline{V}_{\text{coil}}(t) + \left(\underline{R}_{\text{drop}} + \underline{r}_{\text{SNU}}(t)\right) \underline{I}_{\text{coil}}(t), \quad (2)$$

where $\underline{r}_{\text{SNU}}(t)$ is the SNU resistance, that is not constant during the scenario, and $\underline{R}_{\text{drop}}$ includes all the other resistances in series with the load coil, that can be assumed constant for the present analysis. Moreover, the resistances of the superconducting coils can be neglected.

The voltage present across the PF3 and PF4 terminals during the breakdown phase is the voltage induced by the currents in the other coils.

For each circuit containing a SNU, the corresponding row of $\underline{V}_{\text{PS}}(t)$ is the voltage to be produced by the Base PS during the whole scenario except the breakdown phase, whilst the voltage at the breakdown depends also on the resistance R_{SNU} inserted by the SNU. This resistance is a degree of freedom in the PS design. Moving from the criterion of minimizing the PS power, the minimum SNU resistance can be calculated and selected.

The voltage at the SNU terminals has to raise quickly and with low jitter. The SNU opening time is practically instantaneous in the model. Thus, the ideal R_{SNU} for each circuit can be calculated from the voltage variation at the breakdown divided by the available coil current:

$$R_{\text{SNU}} = \frac{V_{\text{PS}}(0) - V_{\text{PS}}(\Delta t_0)}{I_{\text{coil}}(0)}, \quad (3)$$

where Δt_0 is a minimal time interval after the conventional time zero given by the breakdown initiation. Normally, several resistance values can be selectable in a SNU. The value obtained by (3) for the maximum PS current provides a reference for the minimum SNU resistance (in the order of hundreds of milliohms for the considered scenario).

For sake of clearness, the difference between V_{PS} and V_{coil} is shown in Fig. 5 for the case of the CS3U module.

The voltage curves in Fig. 6 take into account also the circuit drops and the SNU effects, then they represent the voltage to be generated by each Base PS. The semiconductors and the other bridge components, as well as the step-down transformers, are selected to comply with these values.

2.5. Power scenarios

The instantaneous power generated by the Base PS

$$\underline{P}_{\text{PS}}(t) = \underline{V}_{\text{PS}}(t) \cdot \underline{I}_{\text{PS}}(t) \quad (4)$$

practically corresponds to the active power $P(t)$ absorbed from the grid through the step-down transformers. A small part of this power (about 2%) is dissipated in the connections, in the transformers and in the thyristor junctions.

The thyristor bridges can sustain high powers with good reliability but require high reactive power $Q(t)$ to operate. This can be estimated by approximated formulae reported in the technical literature [17, 18].

The active and reactive power scenarios for each coil are shown in Fig. 7. These powers are necessary to produce the current in Fig. 3 with the voltage in Fig. 6.

The impact of the PS systems on the distribution network can be quantified by the apparent power $S(t)$ that is the module of the complex power

$$\vec{S}(t) = P(t) + jQ(t). \quad (5)$$

The total power contribution of the CS, PF and IC PS systems is summarized in Fig. 8. While $P(t)$ has a positive peak of 20 MW, $Q(t)$ can reach about 60 Mvar.

3. Power supplies for the toroidal field coils

The TFC PS system is designed to provide the required DC current to the superconducting coils for an entire experimental period (hours or days). The total coil inductance is about 1.5 H. The flat-top current of 50 kA can be reached by applying a low voltage for a long time. Afterwards, the obtained flat-top current can be maintained for many plasma experiments.

Just to illustrate the involved parameters, Fig. 9 presents a reference situation in which the coils are charged and discharged for a single 100 s experiment. The resulting powers are quite low, if compared with those in Fig. 8, that are instead characterized by a duty cycle of 100s/3600s. In practice, due to the limited values and variations, the TFC power contribution can be taken into account by including it in the auxiliary power described in Section 5.

Since the TFC operations do not require a SNU, only the Base PS controls the voltage. However, some FDUs in series are foreseen to protect groups of TFCs [19]. A polarity changer is being planned to be inserted between the TFC current feeders.

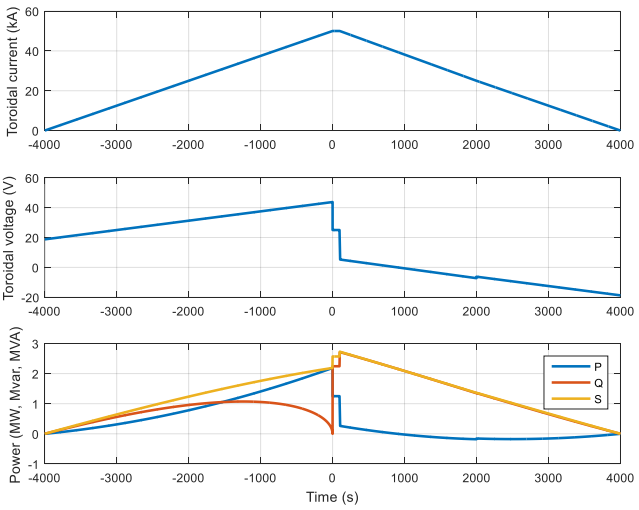

Fig. 9. TFC current, voltage and electric powers when the coils are charged and discharged for a single 100 s experiment.

Table 1

Assumed approximated performances of the additional heating systems considered for the DTT electrical design.

Additional heating system	Power to plasma	Efficiency	Power factor
ICRH	10 MW	60%	0.7
ECRH	15 MW	30%	0.9
P-NBI	0	40%	0.6
N-NBI	20 MW	25%	0.6
Global equivalent	45 MW	35%	0.65

4. Power supplies for additional heating

Even if the heating systems will be upgraded in successive phases, the power contribution related to the additional heating systems has been estimated assuming a total power of 45 MW coupled to the plasma for 100s/3600s [10].

The actual electrical power required to obtain such effect on the plasma depends on the adopted heating system. In the first phase of DTT, a mix of ICRH Ion Cyclotron (klystrons or tetrodes at 60-90 MHz) and ECRH (gyrotrons at 170 GHz) are considered, as indicated by the first two rows in Table 1, while NBI is the most probable way to upgrade the power (N-NBI due to the high plasma density). The approximate performances of such systems are summarized in the Table 1, where some worst-case assumptions and safety margins were introduced. The efficiency considered in the table is the percentage of the active power absorbed from the distribution network that is actually delivered to the plasma.

Considering a mix of additional heating systems upgradable in the future, the pessimistic values 35% and 0.65 were assumed in the last row of Table 1 as the global equivalent efficiency and power factor, respectively.

As shown in Fig. 10, a realistic scenario was assumed for the evolution of the heating power during the experiment: after the breakdown, the power delivered to the plasma is increased with steps of 5 MW/s. A similar progressive reduction is expected in the discharge phase.

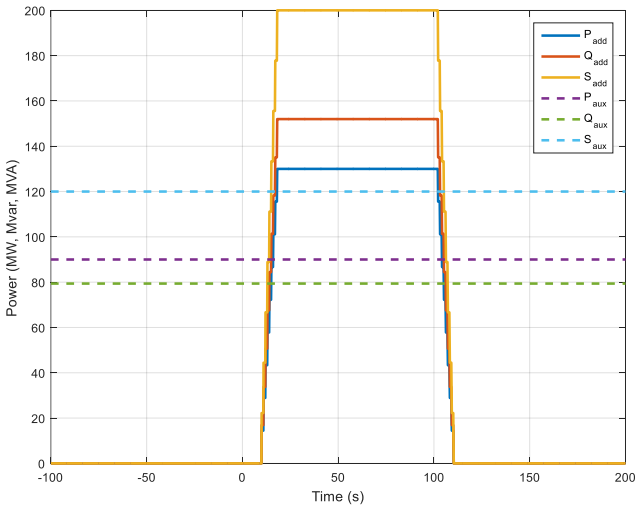

Fig. 10. Power contributions from the additional heating and auxiliary systems.

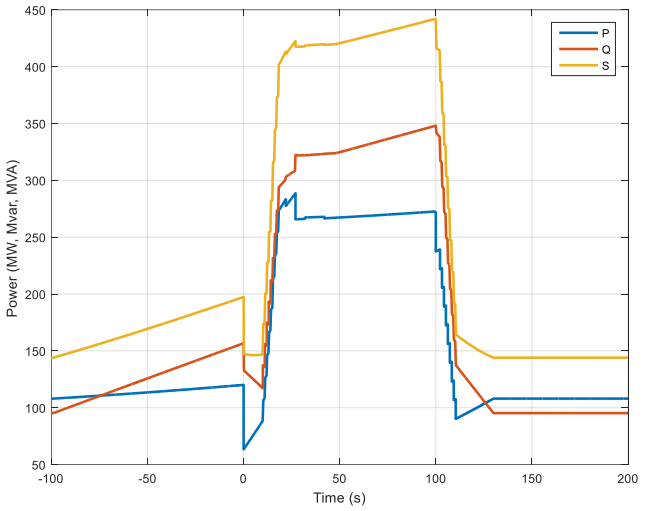

Fig. 11. Total electrical powers of the DTT facility for the reference scenario.

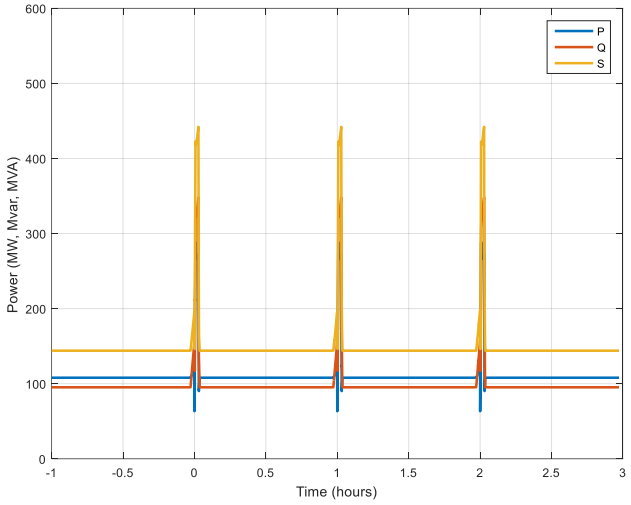

Fig. 12. DTT electrical powers over consecutive experiments at the nominal duty cycle.

5. Auxiliary power supplies

Several auxiliary systems and services are necessary for the DTT operations [2-7]: fueling, vacuum systems, pumps, cooling and cryogenic systems, diagnostics, control and monitoring, remote handling, compressed air and fluid services, communication interfaces, computers, air conditioning and so on.

The contribution from the auxiliary systems was estimated assuming a constant power demand of 90 MW with a power factor of 0.75. This model takes into account also the TFC contributions.

Fig. 10 summarizes the models assumed for the estimation of the contributions due to the additional and auxiliary powers.

6. DTT power scenarios

Fig. 11 shows the total active, reactive and apparent powers resulting from all the contributions described in the previous sections. In order to ensure a good safety margin, a 20% increment was applied on both the estimated active and the reactive powers, so obtaining the power time evolutions in Fig. 11.

It is important to stress that the plant is designed to operate at these power levels with the nominal duty cycle of 100s/3600s. Most of the experimental campaigns, especially in the first months of operations, are expected to be performed at reduced power with shorter times.

Extending the results in Fig. 11, Fig. 12 shows the power profiles for more consecutive experiments during a working day. This is a good model of the most demanding load affecting the national grid and were so submitted to the Italian national grid operator (TERNA) for the required analyses and authorizations (see Section 8.1).

Of course, the graphs report the reactive powers before any intervention for power factor correction to have a general overview of the situation. This topic is addressed in Section 8.2.

7. Preliminary ratings of PS components

The preceding analyses were useful also to identify the preliminary characteristics of the main DTT PS systems and components. Even though further optimization will be possible, an effort was performed to obtain homogenous or modular structures for cost reduction and maintenance simplification. This is summarized by the bars in Fig. 13 and in Fig. 14.

All the Base PSs were designed to operate on 4 quadrants, being able to produce both forward and backward currents, even when it was not strictly necessary looking at the available scenarios (see also Fig. 3). The output current and voltage ratings were mostly divided in classes of ±15, ±20 and ±25 kA, to be implemented by modular 5 kA bridges in parallel.

Except for IC5 and IC6, all the Base PSs are based on 12-pulses self-commutated (thyristor) bridges with circulating current. The expected voltage rating is ±800 V. The IC5 and IC6 PSs are based on IGBT or IGCT devices with ±1 kV output voltage to be fast enough to control the plasma vertical position and to cover a wide range of situations.

While the present ENEA tokamak (FTU) is mostly supplied through flywheels, the DTT PSs are connected to the national grid (see Section 8). This would result in a very stable frequency (50 Hz), reducing the modelling and design problems due to the variable frequency.

Since the SNU resistance values obtained from the calculations introduced in Section 2.4 are quite homogenous and well implementable (similar to those built for JT-60SA [13]), they were used to calculate the voltages produced across the SNU for the current actually flowing at the breakdown. These voltages are compared in Fig. 14 with the SNU nominal voltages. Furthermore, several possible resistance combinations will be available in the final design. In the final design, the voltages of all the 10 SNUs have to rise quickly and with a jitter that is very shorter than 1 ms (that is compatible with the experimental results of the JT-60SA SNUs [20]).

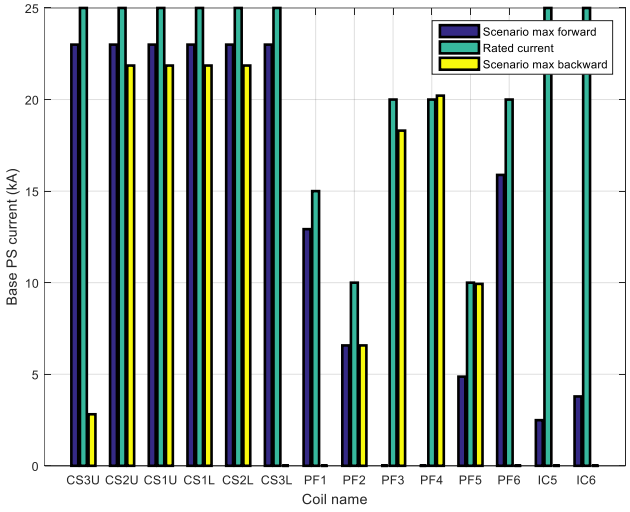

Fig. 13. Comparison between the Base PS rated currents and the values reached in the reference scenario.

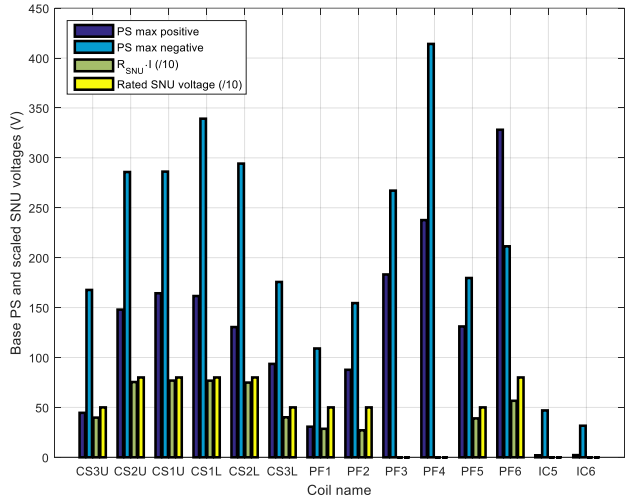

Fig. 14. Voltage reached in the reference scenario by the Base PSs and SNUs compared with the rated SNU voltages (the SNU voltages are scaled for visualization purposes) The coils PF3, PF4, IC5 and IC6 have no SNUs.

Thanks also to the polarity changer, the TFC Base PS can be rated to operate at maximum 50 kA on 2 quadrants with 12 pulses.

The performances in Table 1 can be achieved by high voltage PSs based on IGBTs or MOSFETs and controlled by pulse step modulation [10, 11]. In this case, transformers with multiple secondary windings implement the connection to the medium voltage grid.

As mentioned in the Introduction, all the design choices and selected technologies are expected to be feasible in the available time, even though some of them should reach extremely high performances. However, it is worth noticing that some improvements are under consideration, as the SNU and FDU, whose functions could be unified. Furthermore, an alternative approach based on supercapacitors [21] is being investigated especially for fast PSs as for IC5 and IC6.

8. Electrical distribution system

The ENEA Research Center located in Frascati (close to Rome) is the main candidate as DTT site. This section presents the systems to transmit the electrical power to the Center and to distribute it to the DTT loads.

8.1. Possible connection to the Italian national grid

A new connection to the national extra high voltage (EHV) grid at 400 kV has been foreseen [9] by an intermediate dedicated electric substation 400kV/150kV in proximity to an important node with adequate power. This is also the border of the ENEA property and responsibility. Two underground electric cables would connect the 400kV/150kV substation to another substation 150kV/36kV inside the ENEA Research Center.

Fig. 15 shows a simplified scheme of the DTT PS and electrical distribution systems, considering a 150kV/36kV substation with two 250 MVA transformers. The double path for both the high voltage cables and the substation transformers should ensure a high level of redundancy and reliability. However, the final technical choices are still under discussion.

The map in Fig. 16 shows the main modifications to the ENEA Research Center in Frascati foreseen to upgrade the electrical facilities for DTT. In particular, the electric substation, the converter area and the tokamak building (modified from the FTU hall) are emphasized. The involved areas have been identified, considering the overall dimensions of each electrical device.

8.2. Power factor correction and harmonics limitation

The power factor during the 100 s operation is shown in Fig. 17.

According to the Italian Grid Code, the maximum allowable power factor is 0.75. The target of the DTT design is to continuously correct the power factor to 0.9. The reactive power that has to be compensated is about 220 Mvar. The apparent power peak seen by the national grid is expected to be about 350 MVA.

This could be achieved either by a centralized or by distributed systems. The former solution could use specific static VAR compensators [22] or exploit the existing FTU motor flywheel generator MG3 rated 250 MVA. The main contribution to the latter solution consists in the introduction of a sequential control in the thyristor bridges [23]. The choice among these options is mainly based on economic evaluations.

Some filters will be inserted before the connection to the EHV grid, though the harmonic content is not expected to be excessive thanks to the 12-pulse operations.

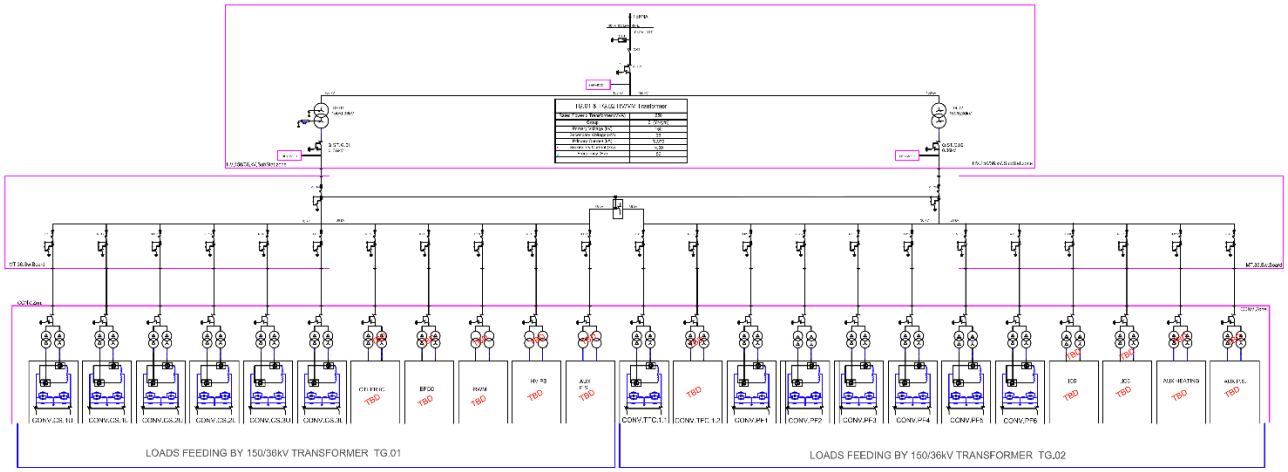

Fig. 15. Preliminary scheme of the DTT electrical distribution and PS system.

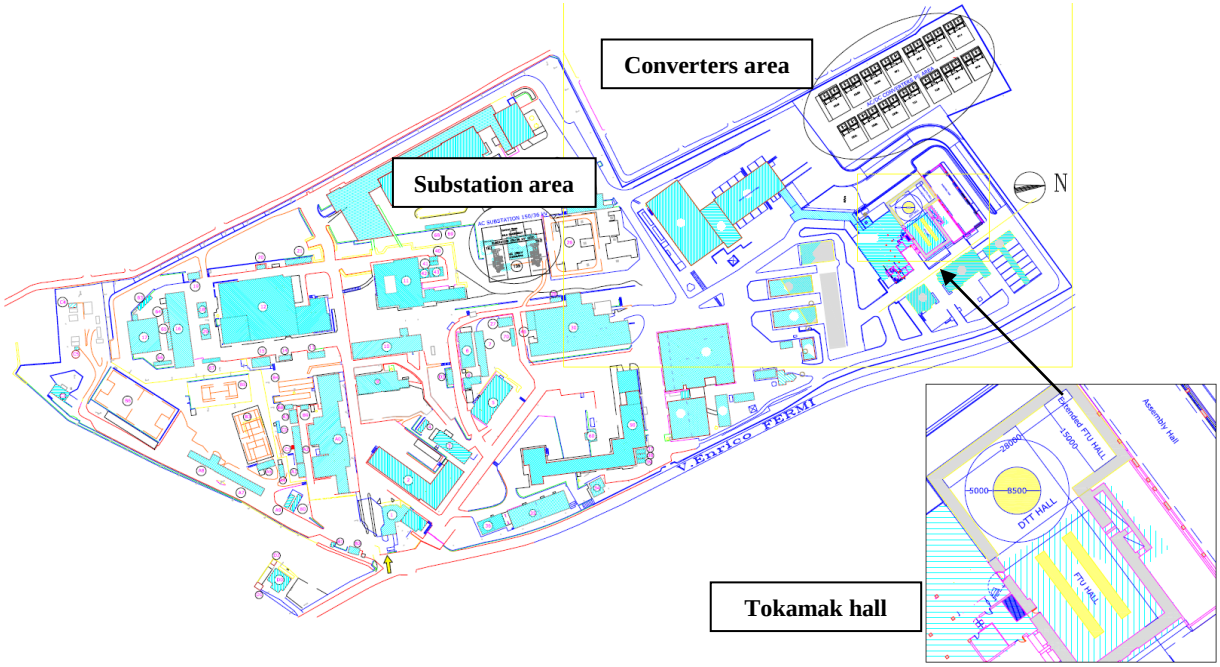

Fig. 16. Map of the Frascati Research Center with emphasis on the main modification for the installation of the DTT electrical facilities.

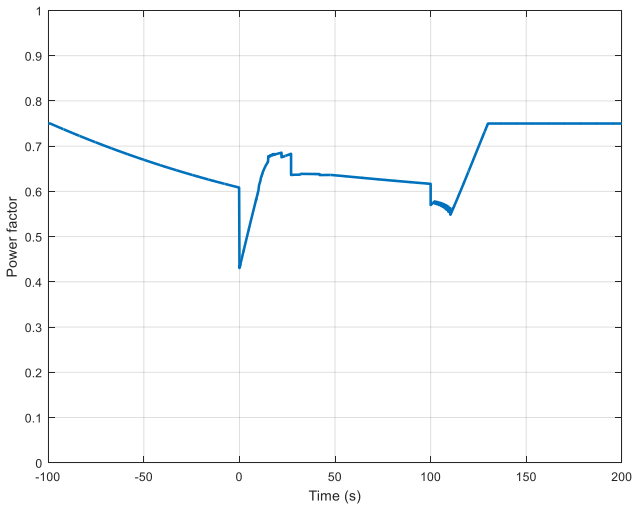

Fig. 17. Instantaneous power factor of the entire DTT plant during the reference scenario.

9. Conclusions

The DTT facility aims to study the power exhaust problem for future experiments and reactors. This requires a complete tokamak with a comprehensive set of PS systems, including at least 30 superconducting coils, about 120 MW for the additional heating systems and almost 100 MW for the auxiliary services.

The voltages, currents and powers to be provided by the PSs were estimated moving from a reference scenario, introducing a reasonable safety margin also to allow modifications and future upgrades. Using these data, the preliminary characteristics of some relevant PS components were identified.

The feasibility of the DTT scenarios at the ENEA Center in Frascati was verified, including a continuous correction of the power factor up to 0.9. The solution identified to supply all the facility directly from the national grid requires the

installation of a new 150 kV cable line specifically for DTT and a new substation with two 150kV/36kV transformers inside the ENEA Center.

The independent evaluation of the electrical requirements of each PS system led to the definition of the active, reactive and apparent power scenarios. Due to the pulsed PSs (serving CS, PFC, IC, ECRH, ICRH, NBI), the 100-MVA permanent load can exceed 400 MVA with a duty cycle of 100s/3600s, but the power factor correction should reduce to 350 MVA the maximum request from the national grid.

Acknowledgement

This work has been carried out within the framework of the EUROfusion Consortium and has received funding from the Euratom research and training programme 2014-2018 under grant agreement No 633053. The views and opinions expressed herein do not necessarily reflect those of the European Commission.

References

[1] EFDA, Fusion Electricity – A roadmap to the realisation of fusion energy, November 2012. Online: http://users.euro-fusion.org/iterphysicswiki/images/9/9b/EFDA_Fusion_Roadmap_2M8JBG_v1_0.pdf

[2] G. Rostagni, The electric power handling from present machines to fusion power stations, Fusion Engineering and Design, Volume 74, Issues 1–4, November 2005, Pages 87–95.

[3] L. Novello, et al., "Advancement on the Procurement of Power Supply Systems for JT-60SA", IEEE 25th Symposium On Fusion Engineering (SOFE), Austin, Texas, USA, May 31-June 4, 2015.

[4] J. Hourtoule, et al., ITER electrical distribution system, IEEE 25th Symposium on Fusion Engineering (SOFE), San Francisco, CA, 2013, pp. 1-5.

[5] S. Nair, J. Hourtoule, K. W. Kang, J. Journeaux, M. Khedekar, Instrumentation and control of the ITER Electrical Power Distribution System, Electrical Machines and Systems (ICEMS), 2013.

[6] C. Neumeyer, et al., ITER power supply innovations and advances, IEEE 25th Symposium on Fusion Engineering (SOFE), San Francisco, CA, 2013, pp. 1-8.

[7] M. Matsukawa, Engineering feature in the design of JT-60SA, Proc. of the 21 Fusion energy 2006, IAEA conference (2007).

[8] F. Crisanti, et al., The DTT device: Rationale for the choice of the Parameters, Fusion Engineering and Design, Special Issue for DTT (2017).

[9] R. Martone et al., The DTT device: costs and management aspects, Fusion Engineering and Design, Special Issue for DTT (2017).

[10] G. Granucci et al., The DTT device: systems for heating, Fusion Engineering and Design, Special Issue for DTT (2017).

[11] P. Zito, et al., A Novel Conceptual Design for Gyrotron's High Voltage Power Supplies, 42nd IEEE Industrial Electronics Conference (IEEE IECON2016), Florence, Italy, 2016.

[12] L. Zanotto, A. Maistrello, L. Novello, V. Toigo, Impact of Consorzio RFX facilities for thermonuclear fusion research on the Italian Extra High Voltage network, Harmonics and Quality of Power (ICHQP), IEEE 15th International Conference on, Hong Kong, 2012, pp. 605-611.

[13] A. Lampasi, A. Coletti, L. Novello, M. Matsukawa, F. Burini, G. Taddia, et al., Final design of the Switching Network Units for the JT-60SA Central Solenoid, Fusion Eng. Des. 89 (2014) 342-348.

[14] E. Gaio, A. Ferro, L. Novello, M. Matsukawa, Power Amplifiers Based on SiC Technology for MHD Mode Control in Fusion Experiments, IEEE Transactions on Plasma Science, no.99, pp.1-8.

[15] P. Zito, et al., Design and realization of JT-60SA Fast Plasma Position Control (FPPC) Power Supplies, Fusion Engineering and Design, Volumes 98–99, October 2015, Pages 1191-1196.

[16] A. Maistrello, et al., Experimental qualification of the Hybrid Circuit Breaker developed for JT-60SA Quench Protection Circuits, IEEE Transactions on Applied Superconductivity, 2014, Volume: 24, Issue: 3.

[17] G. Moltgen, Converter Engineering. An Introduction to Operation and Theory, Siemens, John Wiley and Sons, 1984.

[18] A. Kloss, A basic Guide to Power Electronics, John Wiley and Sons, 1984.

[19] L. Novello, et al., Analysis of Maximum Voltage Transient of JT-60SA Toroidal Field Coils in Case of Fast Discharge, IEEE Transactions on Applied Superconductivity, vol. 26, no. 2, pp. 1-7, March 2016.

[20] A. Lampasi, et al., First Switching Network Unit for the JT-60SA superconducting Central Solenoid, Fusion Engineering and Design, Volumes 98–99, October 2015, Pages 1098-1102.

[21] A. Lampasi, G. Maffia, G. Taddia, S. Tenconi, P. Zito, ETHICAL: A Modular Supercapacitor-Based Power Amplifier for High-Current Arbitrary Generation, 16th IEEE International Conference on Environment and Electrical Engineering (EEEIC), Florence, Italy, 7–10 June 2016.

[22] C. Finotti, E. Gaio, I. Song, J. Tao, I. Benfatto, Improvement of the dynamic response of the ITER Reactive Power Compensation system, Fusion Engineering and Design, 98–99, October 2015, Pages 1058–1062.

[23] K. Shimada, et al., Minimization of Reactive Power Fluctuation in JT-60SA Magnet Power Supply, Plasma Science and Technology, Vol.15, No.2, Feb. 2013.